

# Studies of the Uptake of Nitrate in Barley<sup>1</sup>

## V. Estimation of Root Cytoplasmic Nitrate Concentration Using Nitrate Reductase Activity—Implications for Nitrate Influx

Bryan J. King\*, M. Yaesh Siddiqi, and Anthony D. M. Glass

Department of Botany, University of British Columbia, Vancouver, British Columbia, Canada V6T 1Z4

### ABSTRACT

The cytoplasmic  $\text{NO}_3^-$  concentration ( $[\text{NO}_3^-]_c$ ) was estimated for roots of barley (*Hordeum vulgare* L. cv Klondike) using a technique based on measurement of *in vivo* nitrate reductase activity. At zero external  $\text{NO}_3^-$  concentration ( $[\text{NO}_3^-]_o$ ),  $[\text{NO}_3^-]_c$  was estimated to be 0.66 mM for plants previously grown in 100  $\mu\text{M}$   $\text{NO}_3^-$ . It increased linearly with  $[\text{NO}_3^-]_o$  between 2 and 20 mM, up to 3.9 mM at 20 mM  $[\text{NO}_3^-]_o$ . The values obtained are much lower than previous estimates from compartmental analysis of barley roots. These observations support the suggestion (MY Siddiqi, ADM Glass, TJ Ruth [1991] J Exp Bot 42: 1455–1463) that the nitrate reductase-based technique and compartmental analysis determine  $[\text{NO}_3^-]_c$  for two separate pools; an active, nitrate reductase-containing pool (possibly located in the epidermal cells) and a larger, slowly metabolized storage pool (possibly in the cortical cells), respectively. Given the values obtained for  $[\text{NO}_3^-]_c$  and cell membrane potentials of  $-200$  to  $-300$  mV (ADM Glass, JE Schaff, LV Kochian [1992] Plant Physiol 99: 456–463), it is very unlikely that passive influx of  $\text{NO}_3^-$  is possible via the high-concentration, low-affinity transport system for  $\text{NO}_3^-$ . This conclusion is consistent with the suggestion by Glass *et al.* that this system is thermodynamically active and capable of transporting  $\text{NO}_3^-$  against its electrochemical potential gradient.

The uptake of  $\text{NO}_3^-$ , like that of other ions, appears to be mediated by at least two distinct systems in barley (*Hordeum vulgare* L.) and other higher plants (10, 11, 29, 31 and references therein). The first is an inducible HATS<sup>2</sup>, which has a low  $K_m$  for  $\text{NO}_3^-$ , shows Michaelis-Menten saturation kinetics, is sensitive to metabolic inhibitors, is regulated according to the plant nitrogen status, and appears to be an active transport system (see review by Clarkson [6]).

<sup>1</sup> This research was supported by a Natural Sciences and Engineering Research Council of Canada research grant to A.D.M.G. B.J.K. acknowledges the support of Natural Sciences and Engineering Research Council of Canada and Izaak Walton Killam Memorial Postdoctoral Fellowships (University of British Columbia).

<sup>2</sup> Abbreviations: HATS, high-affinity  $\text{NO}_3^-$  transport system;  $E^N$ , Nernst membrane electrical potential difference; FAD, flavin adenine dinucleotide; LATS, low-affinity  $\text{NO}_3^-$  transport system;  $[\text{NO}_3^-]_c$ , cytoplasmic  $\text{NO}_3^-$  concentration;  $[\text{NO}_3^-]_o$ , external nitrate concentration; NR, nitrate reductase; NRA, nitrate reductase activity;  $\Delta\Psi$ , cell membrane electrical potential difference.

The second system is a constitutive LATS, which operates at higher external  $\text{NO}_3^-$  concentrations, shows linear kinetics, and is considerably less sensitive to metabolic inhibitors. The LATS, therefore, has some of the characteristics that would be expected of an energetically passive, channel-mediated transport system (see review of plant ion channels by Hedrich and Schroeder [15]) that facilitates the movement of  $\text{NO}_3^-$  down its electrochemical potential gradient.

The direction of  $\text{NO}_3^-$  transport through such a passive system depends upon the electrochemical potential difference for nitrate. This is determined by three factors:  $[\text{NO}_3^-]_o$ ,  $[\text{NO}_3^-]_c$ , and the cell membrane electrical potential difference,  $\Delta\Psi$ .  $[\text{NO}_3^-]_c$  has been estimated in several studies, using various methods. The technique of compartmental analysis has been applied to roots of several plant species using the tracer <sup>13</sup>N or <sup>15</sup>N, subsequent to the early work of Deane-Drummond and Glass (8) using <sup>36</sup>ClO<sub>3</sub><sup>-</sup>. Presland and McNaughton (24) and Lee and Clarkson (18), using <sup>13</sup>N, obtained values of 50 to 100 and 26 mM for maize and barley roots, respectively. Macklon *et al.* (20), using <sup>15</sup>N, obtained values of 40 to 50 mM in onion roots. Siddiqi *et al.* (29), using <sup>13</sup>N, found that  $[\text{NO}_3^-]_c$  in barley roots increased from 12 to 37 mM with increased  $[\text{NO}_3^-]_o$  from 0.01 to 1 mM.

Miller and Zhen (23), using  $\text{NO}_3^-$ -specific microelectrodes, estimated  $[\text{NO}_3^-]_c$  in *Chara* cells to be 1.6 mM. Recently, Zhen *et al.* (33) applied a similar technique to barley roots, obtaining values of 5.4 and 3.2 mM for  $[\text{NO}_3^-]_c$  in epidermal and cortical cells, respectively.

In contrast, Robin *et al.* (25) estimated  $[\text{NO}_3^-]_c$  in leaves of pea, soybean, alfalfa, barley, maize, and rice using the *in vivo* rates of NRA under anaerobic conditions and obtained estimates ranging from approximately 10 to 100  $\mu\text{M}$ . Belton *et al.* (3) used this method to analyze the data of Brunetti and Hageman (4) for whole wheat plants and that of Jordan and Fletcher (16) for cultured rose cells. They obtained values of 65 and 140  $\mu\text{M}$ , respectively. Using <sup>14</sup>N NMR, the same authors estimated  $[\text{NO}_3^-]_c$  to be quite low compared with the vacuolar  $[\text{NO}_3^-]$  in barley, maize, and pea roots, although the precise value could not be determined by this method.

It is evident that the estimates of  $[\text{NO}_3^-]_c$  from compartmental analysis and  $\text{NO}_3^-$ -specific microelectrodes are 2 to 3 orders of magnitude higher than those obtained with the NR-based technique of Robin *et al.* (25). Siddiqi *et al.* (31) proposed that  $[\text{NO}_3^-]_c$  is a critical factor in determining whether passive  $\text{NO}_3^-$  uptake via the LATS is possible. If

$[\text{NO}_3^-]_c$  is in the millimolar range as suggested by compartmental analysis, passive influx of  $\text{NO}_3^-$  via the LATS would be essentially impossible, requiring a positive value for  $\Delta\Psi$  (31). However, if it is in the micromolar range as suggested by the NR-based method, passive transport might be possible given  $\Delta\Psi$  values from approximately  $-50$  to  $-100$  mV (31).

Siddiqi *et al.* (29) proposed a model, based on studies of barley roots, to reconcile the results of compartmental analysis with those of the NR-based method and with the apparently passive characteristics of the LATS. They suggested that compartmental analysis measures  $[\text{NO}_3^-]_c$  primarily in the root cortical cells, whereas the method based on NRA measures  $[\text{NO}_3^-]_c$  of epidermal cells. The cytoplasm of the cortical cells may serve as a pool for unmetabolized  $\text{NO}_3^-$  (29), which is eventually either effluxed to the external medium or translocated to the shoot (21), and  $[\text{NO}_3^-]_c$  in this pool might be in the millimolar range (29). Recently supplied  $\text{NO}_3^-$ , however, may be reduced in a separate epidermal pool (29) or translocated to the shoot (21), and, indeed, in corn roots the majority of NR appears to occur in the epidermis (27). The presence of NR in the epidermal cells and a rapid rate of  $\text{NO}_3^-$  turnover might maintain  $[\text{NO}_3^-]_c$  at a micromolar level, sufficiently low for passive influx of  $\text{NO}_3^-$  to occur via the LATS (31).

Recently, however, Glass *et al.* (10), using microelectrodes, measured  $\Delta\Psi$  values ranging from  $-200$  to  $-300$  mV in epidermal and cortical root cells of barley. For the LATS to allow passive  $\text{NO}_3^-$  uptake into the cells under such conditions at typical  $[\text{NO}_3^-]_o$  values, they calculated that  $[\text{NO}_3^-]_c$  would have to be in the nanomolar range, much lower than the estimates of any previous studies. Furthermore, they observed that transport via the LATS caused depolarization of  $\Delta\Psi$ , which is not consistent with a passive channel-mediated mechanism. They proposed, instead, that the LATS is an active, electrogenic system, possibly involving cotransport with  $\text{H}^+$ .

In light of the discrepancy between estimates of  $[\text{NO}_3^-]_c$  obtained with the NR-based method and those obtained using compartmental analysis, we decided to estimate  $[\text{NO}_3^-]_c$  of barley roots using the NR-based method (25). In earlier papers in this series, we described the kinetics, energetics, and electrophysiology of the LATS and HATS in barley roots (10, 11, 31) and compartmental analysis of  $\text{NO}_3^-$  in the root cells (29). In the present study, we have compared the results from the NR-based method with those obtained for barley by Siddiqi *et al.* (29) using compartmental analysis. Our goal was to determine whether  $[\text{NO}_3^-]_c$  is sufficiently low in  $\text{NO}_3^-$ -reducing cells to allow passive  $\text{NO}_3^-$  transport into these cells via the LATS, given the  $\Delta\Psi$  values obtained for barley roots by Glass *et al.* (10). The study constitutes an evaluation of the contrasting hypotheses of Siddiqi *et al.* (29) and Glass *et al.* (10) referred to above, using the same barley variety grown under similar conditions. The study provides further evidence regarding the nature of the LATS for  $\text{NO}_3^-$  in barley roots.

## MATERIALS AND METHODS

### Seed Germination and Plant Growth

Seeds of barley (*Hordeum vulgare* L. cv Klondike) were germinated in the dark in moist sand on plastic mesh fitted

into Plexiglas discs (approximately 40 seeds per disc) as described by Siddiqi and Glass (28). After 3 d, the discs were transferred to 25-L Plexiglas hydroponic tanks containing  $\frac{1}{80}$ -strength modified Johnson's nutrient solution (30) with  $100 \mu\text{M}$   $\text{NO}_3^-$  supplied as  $\text{Ca}(\text{NO}_3)_2$  and grown for 4 d.  $\text{NO}_3^-$  and  $\text{K}^+$  concentrations were monitored daily, and the nutrient supply was maintained by means of peristaltic pumps, with the delivery rate adjusted according to the rate of  $\text{NO}_3^-$  depletion. The plants were maintained in a controlled environment room at  $20 \pm 2^\circ\text{C}$  with a 16-h light/8-h dark cycle and 70% RH. The light was provided by fluorescent tubes having a spectral composition similar to that of sunlight, at an intensity of  $300 \mu\text{E m}^{-2} \text{s}^{-1}$  at plant level.

### Spectrophotometric Assays

$\text{NO}_2^-$  was assayed essentially as described by Long and Oaks (19) except that the reagents were added at higher concentrations to reduce volume and improve the sensitivity. *N*-1-Naphthylene-diamine-dihydrochloride (0.25 mL of 0.08% [w/v]) and sulfanilamide (0.5 mL of 2% [w/v] dissolved in 5 N HCl) were added to 1.5 mL of sample in a 10-mL test tube and mixed. The sample was allowed to stand at least 30 min, and then  $A_{540}$  was measured spectrophotometrically. High  $\text{NO}_3^-$  concentrations were found to give a slight color reaction in this assay, so this interference was corrected for when necessary by subtracting a blank containing the appropriate  $\text{NO}_3^-$  concentration.

$\text{NO}_3^-$  was assayed essentially according to the procedure of Cataldo *et al.* (5), involving nitration of salicylic acid under acidic conditions. The sample (0.1 mL) was added to 0.4 mL salicylic acid (w/v, dissolved in concentrated  $\text{H}_2\text{SO}_4$ ), mixed, and allowed to stand for 20 min at room temperature; then 9.5 mL of 2 N NaOH was added slowly with mixing. The samples were allowed to cool, and then  $A_{410}$  was determined spectrophotometrically.

Protein was determined using Coomassie blue G-250 (Protein Assay kit, Bio-Rad, Mississauga, Ontario). The assay reagent (0.2 mL) was added to 0.1 mL sample and 0.7 mL water, and mixed, and the  $A_{595}$  was determined spectrophotometrically.

### In Vivo NR Assay

*In vivo* NRA was measured by anaerobic incubation of excised roots using a method similar to that of Robin *et al.* (26) (see review of Beevers and Hageman [2] for general discussion). Four milliliters of 100 mM  $\text{KPO}_4$  buffer (pH 7.7) containing the desired concentration of  $\text{KNO}_3$  was added to each of several 10-mL Vacutainer tubes (Becton-Dickinson, Rutherford, NJ) and equilibrated in a water bath at  $27 \pm 1^\circ\text{C}$ . Approximately 0.3 to 0.5 g fresh weight of roots were excised, rinsed with  $50 \mu\text{M}$   $\text{CaSO}_4$ , and placed in each tube. The tubes were capped and purged for 5 min with helium, which was introduced through each cap septum by 20-gauge 3.5-inch spinal needles (Becton-Dickinson) connected by a manifold to a compressed gas cylinder. The tubes were returned to the water bath and incubated for the desired period. They were then uncapped and placed in a boiling water bath for 10 min to extract tissue  $\text{NO}_2^-$ , and a 1.5-mL sample was withdrawn and assayed for  $\text{NO}_2^-$  as described above. The root fresh

weight was determined, and NRA was expressed as  $\mu\text{mol NO}_2^- \text{ g}^{-1}$  fresh weight  $\text{h}^{-1}$ .

### In Vitro NR Assay

This procedure was carried out essentially according to the method of Long and Oaks (19). For the extraction procedure, barley roots were placed in a mortar kept on ice, ground in liquid nitrogen, transferred to precooled vials, and stored at  $-80^\circ\text{C}$  for later use (within 1–2 d). Approximately 5 g of frozen powder was ground with 5 mL of chilled extraction buffer in a mortar on ice and filtered through nylon mesh into a small beaker. The extraction buffer (17) contained Tris-HCl (25 mM, pH 8.5), EDTA (1 mM), FAD (20  $\mu\text{M}$ ), BSA (1%, w/v), DTT (1 mM), and cysteine (10 mM). Chymostatin (dissolved in DMSO; final concentration 10  $\mu\text{M}$ ) was added as a protease inhibitor, which is known to stabilize NRA extracted from maize roots (19). After extraction, the filtrate volume was determined, and the filtrate was centrifuged at 45,000g for 45 min at  $4^\circ\text{C}$ . The sample supernatant was kept on ice before subsequent steps.

To determine the  $\text{NO}_3^-$  concentration dependence of NRA, it was necessary to remove endogenous  $\text{NO}_3^-$  from the extracted samples by gel filtration, because a large amount of  $\text{NO}_3^-$  (amounting to 3–4 mM in the final extract) was released from the vacuole during grinding of the tissue. A 16- $\times$  2-cm column of coarse mesh Sephadex G-25 (Pharmacia) was equilibrated with approximately 200 mL of 25 mM Tris HCl (pH 8.5) and then with 50 mL of the extraction buffer as described above but modified by the omission of BSA and FAD. Approximately 10 mL of the sample supernatant was applied to the column, and elution was carried out with an additional 50 mL of modified extraction buffer to elute soluble proteins, followed by approximately 100 mL of 25 mM Tris HCl. Fractions of 1.5 mL were collected in microcentrifuge tubes and assayed for protein,  $\text{NO}_3^-$ , and NRA.

All of the NRA (amounting to approximately 80% of the activity of the original extract) was eluted with the soluble protein within a volume of 40 mL, and  $\text{NO}_3^-$  was eluted much later, well separated from the protein peak. Therefore, in subsequent experiments, the protein-containing fractions were pooled and stored on ice before NRA was assayed at various  $\text{NO}_3^-$  concentrations.

NRA was assayed essentially as described by Long and Oaks (19). For each assay, 0.2 mL of Hepes buffer (0.65 M, pH 7.0), 0.14 mL FAD (0.2  $\mu\text{M}$ ), and 0.2 mL of  $\text{KNO}_3$  solution (from concentrated stocks according to the desired final concentration) were added to 10-mL test tubes. A predetermined volume of water was added to give a final volume of 1.4 mL for incubation after the sample and other reagents were added, and the mixture was equilibrated in a water bath at  $28 \pm 1^\circ\text{C}$ . An aliquot of sample, typically 0.4 to 0.5 mL, was added, and the reaction was started by the addition of 0.1 mL of NADH (3.6 mg  $\text{mL}^{-1}$ ) with mixing. The tubes were incubated at  $28^\circ\text{C}$  for 30 min, and then the reaction was stopped by boiling for 10 min. The tubes were cooled to  $28^\circ\text{C}$ , and 0.1 mL of pyruvic acid (5.3 g  $\text{L}^{-1}$ ) and 2  $\mu\text{L}$  of lactate dehydrogenase suspension (Boehringer-Mannheim, Montreal, PQ) were added with mixing. An additional 10-

min incubation was carried out to oxidize residual NADH, which interferes with color development in the  $\text{NO}_2^-$  assay (19). The samples were then assayed for  $\text{NO}_2^-$  as described above.

In one experiment, NRA was assayed at various  $\text{NO}_3^-$  concentrations using NADPH as the electron donor. In this case, 0.1 mL of NADPH (2.64 mg  $\text{mL}^{-1}$ ) was added to start the reaction instead of NADH, and lactate dehydrogenase and pyruvate were included during the incubation with NADPH to eliminate any NADH produced by phosphatase action on NADPH (32). The slight interference of NADPH with color development in the  $\text{NO}_2^-$  assay was corrected for by including the same concentration of NADPH when running  $\text{NO}_2^-$  standards.

### Terminology and Calculations

The *in vitro* NRA determined with NADH as the sole electron donor is referred to in the text and figures as "total activity," because this includes activity due to an NADH-specific NR and an NAD(P)H-bispecific NR (19, 32, and references therein). The activity obtained with NADPH alone can be attributed to the NAD(P)H-bispecific enzyme and is referred to here as "NADPH activity." Activity due to the NADH-dependent form ("NADH activity") is obtained by subtraction of the NADPH activity from the total activity.

The  $K_m$  and  $V_{\text{max}}$  for  $\text{NO}_3^-$  for the NADH and NAD(P)H enzymes were determined by Eadie-Hofstee analysis of the NADH and NADPH activities. The rate of *in vivo* NRA due to the NADH-specific enzyme ( $V$ ) at various external  $\text{NO}_3^-$  concentrations ( $[\text{NO}_3^-]_o$ ) was estimated by subtraction of the NADPH activity, which was considered to be saturated at all values of  $[\text{NO}_3^-]_o$  (see "Discussion"). The  $[\text{NO}_3^-]_c$  was then determined for various values of  $[\text{NO}_3^-]_o$  by rearranging the Michaelis-Menten equation:

$$[\text{NO}_3^-]_c = \frac{V \cdot K_m}{V_{\text{max}} - V}$$

This value was then compared to that obtained theoretically from the Nernst equation at  $20^\circ\text{C}$  for various values of  $[\text{NO}_3^-]_o$  and  $\Delta\Psi$ , assuming passive equilibration of  $\text{NO}_3^-$  (in which case  $E^N = \Delta\Psi$ ):

$$[\text{NO}_3^-]_c = [\text{NO}_3^-]_o \cdot 10^{(E^N/(RT/zF))}$$

where  $R$  represents the gas constant;  $T$ , temperature (K);  $z$ , the charge of the ion; and  $F$ , the Faraday constant.

### RESULTS

Figure 1 shows the *in vivo* production of  $\text{NO}_2^-$  due to NRA of excised barley roots incubated anaerobically during a 6-h period in the presence and absence of exogenous  $\text{NO}_3^-$  (100 mM  $[\text{NO}_3^-]_o$ ). For both treatments,  $\text{NO}_2^-$  accumulation was most rapid in the first 20 to 30 min (Fig. 1, inset). The rates of NRA, calculated by regression of the mean values during the first 20-min period, were  $0.77 \pm 0.08$  and  $1.04 \pm 0.17$   $\mu\text{mol g}^{-1}$  fresh weight  $\text{h}^{-1}$  ( $n = 4$ ) for the  $-\text{NO}_3^-$  and  $+\text{NO}_3^-$

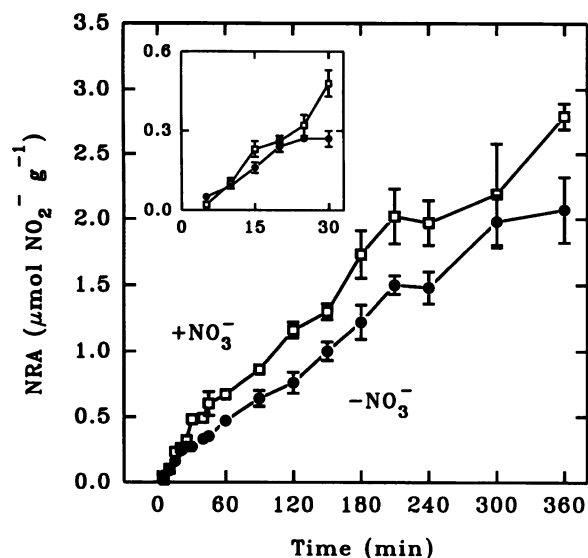


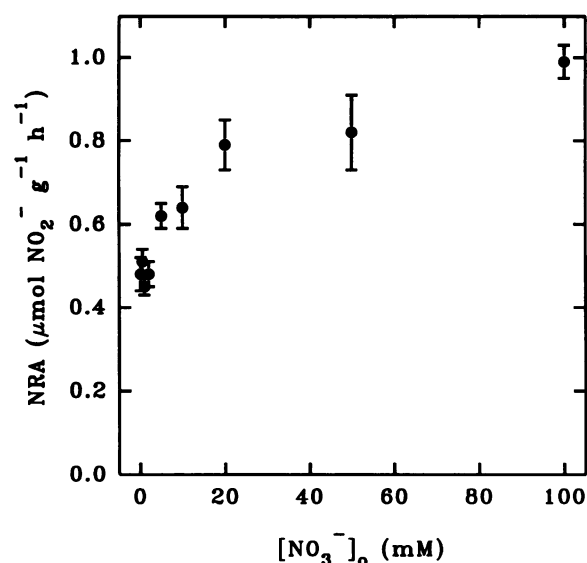
**Figure 1.** Time course of *in vivo* NRA of excised barley roots incubated under anaerobic conditions in the presence ( $\square$ ) and absence ( $\bullet$ ) of exogenously supplied  $\text{NO}_3^-$  (100 mM). Each point is the mean  $\pm$  SE of four to ten replicates. The inset shows the pattern of NRA during the first 30 min period, with symbols as above.

treatments, respectively. Subsequently, the rates were lower, with  $\text{NO}_2^-$  production continuing in a linear pattern until 3.5 h, at an average rate of  $0.39 \pm 0.01$  and  $0.50 \pm 0.02 \mu\text{mol g}^{-1}$  fresh weight  $\text{h}^{-1}$  ( $n = 9$ ) for the two treatments, respectively. Between 3.5 and 6 h, the pattern was more variable. For both treatments, some samples continued to produce  $\text{NO}_2^-$  at a considerable rate, whereas in others,  $\text{NO}_2^-$  production declined to near zero. Furthermore, between 1.5 and 6 h,  $\text{NO}_3^-$  was lost from the tissue of the  $-\text{NO}_3^-$  samples to the surrounding medium at a rate of  $0.85 \pm 0.03 \mu\text{mol g}^{-1}$  fresh weight  $\text{h}^{-1}$  ( $n = 4$ ). Because of the high  $\text{NO}_3^-$  background in the medium, it was not possible to determine whether there was also  $\text{NO}_3^-$  efflux from the  $+\text{NO}_3^-$  samples.

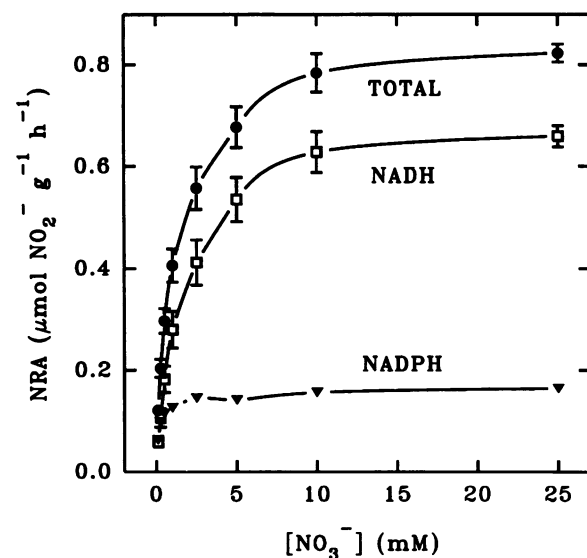
At all times except the earliest (5 min), NRA was considerably higher in the presence of 100 mM  $[\text{NO}_3^-]_0$  than in its absence (Fig. 1), although the magnitude of the differences was variable and failed to show a clear trend with time. Averaged over the period from 10 min to 6 h, NRA for the  $+\text{NO}_3^-$  treatment was  $25.8\% \pm 2.7\%$  ( $n = 14$ ) higher than the  $-\text{NO}_3^-$  rate.

Figure 2 illustrates the  $[\text{NO}_3^-]_0$  dependence of NRA *in vivo*, based on measurement of  $\text{NO}_2^-$  production of excised roots incubated anaerobically for 20 min. The four lowest  $[\text{NO}_3^-]_0$  values used (0.1, 0.5, 1, and 2 mM) were not significantly different in NRA relative to that at zero  $[\text{NO}_3^-]_0$  ( $0.57 \pm 0.03 \mu\text{mol g}^{-1}$  fresh weight  $\text{h}^{-1}$ ;  $n = 18$ ). However, higher  $[\text{NO}_3^-]_0$  (5–100 mM) resulted in higher rates of NRA, with the maximum rate ( $0.99 \pm 0.04 \mu\text{mol g}^{-1}$  fresh weight  $\text{h}^{-1}$ ;  $n = 18$ ) obtained at 100 mM  $[\text{NO}_3^-]_0$ . Concentrations higher than 100 mM were strongly inhibitory, with a  $70\% \pm 16\%$  ( $n = 18$ ) reduction of NRA occurring at 500 mM  $[\text{NO}_3^-]_0$  relative to that at 100 mM.

The *in vitro*  $\text{NO}_3^-$  concentration dependencies of total NRA



**Figure 2.** The effect of exogenous  $\text{NO}_3^-$  on *in vivo* NRA of excised barley roots incubated under anaerobic conditions for 20 min. Each point is the mean  $\pm$  SE of 18 replicates from three separate experiments of six replicates each.



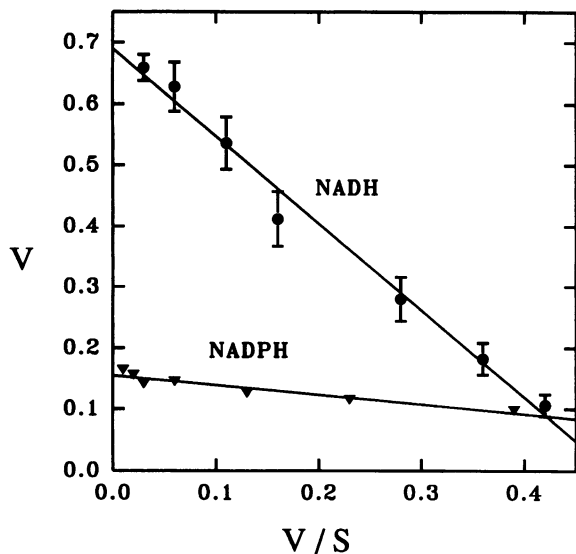
**Figure 3.** The  $\text{NO}_3^-$  concentration dependence of *in vitro* NRA.  $\bullet$ , Total NRA (nine replicates  $\pm$  SE derived from three separate experiments of three replicates each);  $\square$  and  $\blacktriangledown$ , the estimated NADH- and NADPH-dependent NRA, respectively, as explained in "Materials and Methods." The NADPH curve represents the mean of three replicates; SE is smaller than the dimensions of the symbols. The NADH curve was obtained by subtraction of NADPH-dependent activity from the total activity at each  $\text{NO}_3^-$  concentration.

and the NADH- and NADPH-dependent activities are shown in Figure 3. All three curves showed saturation kinetics, with the maximum rates obtained at 25 mM  $\text{NO}_3^-$ . Concentrations higher than 25 mM were somewhat inhibitory (data not shown), with 100 mM resulting in a  $25\% \pm 5\%$  ( $n = 9$ ) reduction of the total NRA relative to that at 25 mM, and in a corresponding reduction of the NADH- and NADPH-dependent activities.

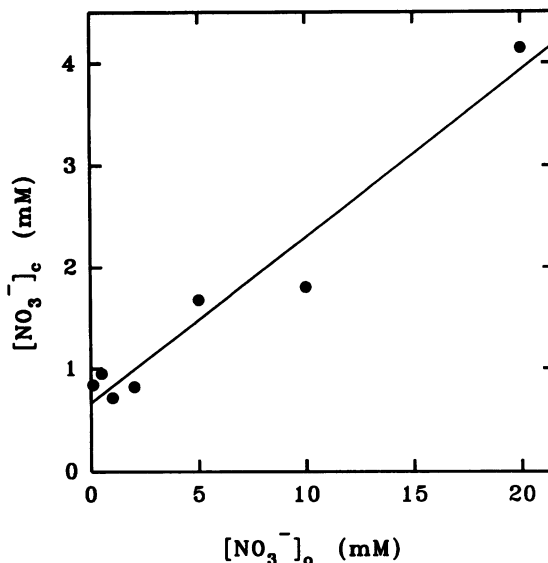
Eadie-Hofstee analysis of the data for total NRA from Figure 3 revealed biphasic kinetics (data not shown), suggesting the presence of more than one NR component. Therefore, kinetic parameters were determined separately for the NADH- and NADPH-dependent activities rather than for the total activity. Figure 4 is an Eadie-Hofstee plot of the NADH- and NADPH-dependent activities from Figure 3, both of which showed a much better straight line fit than the total activity. The  $K_m$  values for  $\text{NO}_3^-$  were 1.41 and 0.16 mM and the  $V_{\max}$  values, 0.69 and  $0.15 \mu\text{mol g}^{-1}$  fresh weight  $\text{h}^{-1}$ , for the NADH- and NADPH-dependent activities, respectively (see Fig. 4 legend for  $\text{SE}$  and  $r^2$  values).

Figure 5 shows the relationship between  $[\text{NO}_3^-]_o$  and the predicted values for  $[\text{NO}_3^-]_c$ , calculated for nonsaturating values of  $[\text{NO}_3^-]_o$ , as described in "Materials and Methods." At zero  $[\text{NO}_3^-]_o$  (the  $y$  intercept),  $[\text{NO}_3^-]_c$  was 0.66 mM, and it increased to 3.9 mM at 20 mM  $[\text{NO}_3^-]_o$ , as determined from the regression line.

Finally, Figure 6 illustrates the logarithmic relationship between  $[\text{NO}_3^-]_c$  and  $E^N$  for four values of  $[\text{NO}_3^-]_o$  from 0.01



**Figure 4.** Eadie-Hofstee analysis of the *in vitro*  $\text{NO}_3^-$  dependence of NRA based on the data shown in Figure 3.  $V$  represents NRA ( $\mu\text{mol g}^{-1}$  fresh weight  $\text{h}^{-1}$ ), and  $S$  represents  $\text{NO}_3^-$  concentration (mM). The  $K_m$  values for  $\text{NO}_3^-$  for the NADH-dependent ( $\bullet$ ) and NADPH-dependent ( $\blacktriangledown$ ) activities, as determined from the slopes, were  $1.41 \pm 0.07$  and  $0.16 \pm 0.02$  mM, respectively, and the  $V_{\max}$  values were  $0.69 \pm 0.03$  and  $0.15 \pm 0.01 \mu\text{mol g}^{-1}$  fresh weight  $\text{h}^{-1}$ , respectively. The  $r^2$  values were 0.99 and 0.91, respectively. The data points for the lowest  $\text{NO}_3^-$  concentration (0.1 mM; not shown) deviated considerably from the rest of the data and were not included in the regression.



**Figure 5.** The relationship between  $[\text{NO}_3^-]_o$  and  $[\text{NO}_3^-]_c$ , based on the data for  $\text{NO}_3^-$  dependence of *in vivo* NADH-dependent NRA, derived from the data shown in Figure 2; a  $K_m$  value for the NADH-dependent activity of 1.41 mM was used, as determined from Figure 4. The slope of the regression line was  $0.16 \pm 0.02$ , and the  $y$  intercept was 0.66. The  $\text{SE}$  of the  $y$  estimates from the regression was 0.30, and the  $r^2$  value was 0.95. The  $\text{SE}$  values of the data used in the calculations are given in Figure 2 and in the legend to Figure 4.

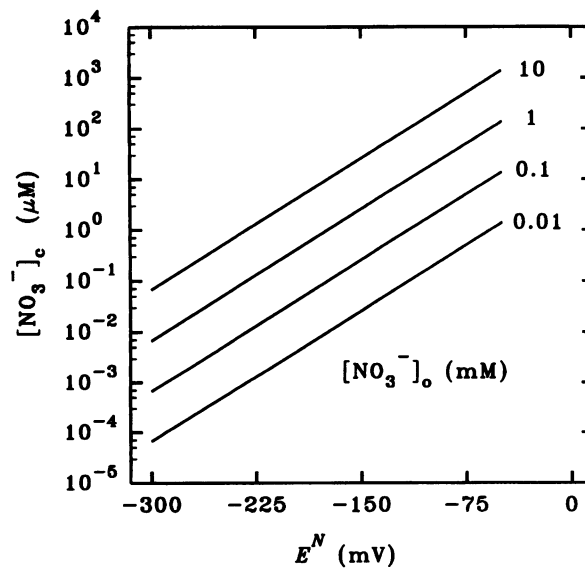


**Figure 6.** The theoretical equilibrium relationship between  $E^N$  and  $[\text{NO}_3^-]_c$  for four values of  $[\text{NO}_3^-]_o$  as calculated from the Nernst equation assuming passive entry of  $\text{NO}_3^-$ .

to 10 mM, as predicted theoretically by the Nernst equation, assuming passive equilibration of  $[\text{NO}_3^-]_o$  and  $[\text{NO}_3^-]_c$  according to  $E^N$ .

## DISCUSSION

### *In Vivo* Nitrate Reduction

Figure 1 demonstrates that excised barley roots incubated under anaerobic conditions are capable of producing  $\text{NO}_2^-$  at substantial rates for at least 6 h in the absence of exogenous  $\text{NO}_3^-$ . Because approximately  $2 \mu\text{mol g}^{-1}$  fresh weight of  $\text{NO}_2^-$  were produced during this time, a  $\text{NO}_3^-$  reserve of at least that magnitude must be present within the roots and available to support NRA. This result agrees with those of Aslam (1) who showed that  $\text{NO}_2^-$  continues to be produced over an 8-h period by leaves of soybean and barley incubated anaerobically, although, as in our system, the rates gradually declined over time. Likewise, Robin *et al.* (25, 26) observed that pea leaves incubated anaerobically produced  $\text{NO}_2^-$  in a linear fashion over a 3-h period, with reductions in rate occurring subsequently.

We observed that, on average, the addition of exogenous  $\text{NO}_3^-$  at 100 mM enhanced  $\text{NO}_2^-$  production by 26% (Fig. 1), in close agreement with the results of Robin *et al.* (25). This result clearly indicates that NRA is limited by the availability of  $\text{NO}_3^-$  under these conditions rather than by reductant supply or other factors. This observation is critical to the interpretation of the data presented here, because to use the NR-based method to estimate  $[\text{NO}_3^-]_c$ , NRA *in vivo* must be  $\text{NO}_3^-$  limited.

Ferrari *et al.* (9), using cultured tobacco cells, found that  $\text{NO}_2^-$  production essentially ceased after 1 h of anaerobic incubation, despite the fact that the total tissue  $\text{NO}_3^-$  was not significantly depleted. The cessation was not due to depletion of reductant supply or other factors, because addition of exogenous  $\text{NO}_3^-$  caused resumption of  $\text{NO}_2^-$  production. Ferrari *et al.* (9) therefore inferred the presence of two  $\text{NO}_3^-$  pools, a metabolic pool (presumably cytoplasmic), which became depleted of  $\text{NO}_3^-$  within a 1-h period but could be replenished by exogenous  $\text{NO}_3^-$ , and a storage pool, presumably vacuolar, which was much larger but inaccessible to the metabolic pool over the time period studied.

Our results and those of Robin *et al.* (25, 26) differ from those of Ferrari *et al.* (9) in that  $\text{NO}_2^-$  production, although limited by  $\text{NO}_3^-$  supply, continued over an extended time period. The successive declines in rates that were observed after 30 min and after 3.5 h occurred in both the presence and absence of exogenous  $\text{NO}_3^-$  and were, therefore, clearly not due to  $\text{NO}_3^-$  limitation.

We believe our results, and those of Robin *et al.* (25), indicate that the vacuolar  $\text{NO}_3^-$  storage pool is readily available to the cytoplasmic pool and is capable of supplying  $\text{NO}_3^-$  so as to maintain NRA at a relatively constant rate. For example, between 30 min and 3.5 h, the accumulation of  $\text{NO}_2^-$  was essentially linear. Under conditions where NRA is limited by  $\text{NO}_3^-$ , this must indicate that  $\text{NO}_3^-$  is being delivered to the metabolic pool at a steady rate; otherwise, changes in NRA should be apparent with time. This idea is supported by previous observations with the same barley

cultivar, showing that the pool of cytoplasmic  $\text{NO}_3^-$  is relatively small and unable by itself to maintain NRA for prolonged periods (29), and that total root  $[\text{NO}_3^-]$  (mainly vacuolar) declines rapidly when external  $\text{NO}_3^-$  is removed (30). It seems quite reasonable that the vacuole should, under conditions of low  $[\text{NO}_3^-]_o$ , be able to deliver  $\text{NO}_3^-$  to maintain the cytoplasmic pool and support NRA.

Three concerns might arise regarding the accuracy of the NRA values obtained using the *in vivo* method. First, the anaerobic treatment might be expected to cause depolarization of the plasma membrane, interfering with the uptake of exogenous  $\text{NO}_3^-$ . This could account for the fact that there was no increase in NRA between 0 and 2 mM  $[\text{NO}_3^-]_o$  (Fig. 2). However, concentrations between 2 and 100 mM clearly caused a significant increase in NRA, indicating that the exogenous  $\text{NO}_3^-$  was able to enter the tissue and allowing an estimate of the maximum *in vivo* NRA to be obtained.

Second, anaerobiosis could have an adverse effect on NRA (for example, by decreasing the reductant supply for NRA). However, the fact that NRA continued for several hours and was  $\text{NO}_3^-$  limited clearly indicates that the reductant supply was not the limiting factor for NRA during the experiments.

Finally, anaerobiosis might not cause complete inhibition of  $\text{NO}_2^-$  reductase activity, resulting in further metabolism of  $\text{NO}_2^-$ , again resulting in an underestimation of NRA (13). To test this possibility, we incubated roots anaerobically with  $^{13}\text{NO}_3^-$  over a 10 min period (see refs. 11 and 29–31 for methodology), boiled the roots to extract the label that was taken up, and separated the cationic fraction from the anionic/neutral fraction by cation exchange under acidic conditions. Essentially all of the label was present in the anionic/neutral fraction, which would comprise mainly  $\text{NO}_3^-$  and  $\text{NO}_2^-$ , and none was in the cationic fraction, which would include  $\text{NH}_4^+$  and amino acids. This indicated that further metabolism of  $\text{NO}_2^-$  was blocked under the conditions we used.

For the above reasons, we believe our study has given reasonable estimates of the true *in vivo* NRA. In support of this statement, the *in vivo* rates of NRA during the first 30 min agree quite well with those obtained by the *in vitro* assay (see below). In any case, even a quite substantial error in our estimates would not significantly alter the conclusions of this study (see final section of "Discussion").

We chose a 20-min incubation period to examine the *in vivo* response of NRA to varying  $[\text{NO}_3^-]_o$  (Fig. 2). NRA showed saturation kinetics, increasing nearly twofold between 0.1 and 100 mM, where the maximum rate was obtained. The curve did not resemble a typical rectangular hyperbola, mostly because substantial rates of NRA (approximately  $0.5 \mu\text{mol g}^{-1}$  fresh weight  $\text{h}^{-1}$ ) were obtained even at low  $[\text{NO}_3^-]_o$  values. This is because, even at zero  $[\text{NO}_3^-]_o$ ,  $[\text{NO}_3^-]_c$  can be maintained at a level that supports NRA for extended periods due to the vacuolar flux, as explained above.

The results are similar to those obtained by Robin *et al.* (25) except that we found that  $[\text{NO}_3^-]_o$  values higher than 100 mM were inhibitory, whereas in their study full NRA was obtained up to nearly 1 M. Our results clearly show that, with a 20-min anaerobic incubation,  $[\text{NO}_3^-]_c$  is limiting for NRA.

### In Vitro Nitrate Reduction

Figure 3 shows the *in vitro* dependence of NRA on  $\text{NO}_3^-$  concentration for the total activity and the NADH- and NADPH-dependent activities, which were determined as described in "Materials and Methods." The total activity approached saturation at 25 mM  $\text{NO}_3^-$ , with a rate of approximately  $0.8 \mu\text{mol g}^{-1}$  fresh weight  $\text{h}^{-1}$ . This compares favorably with the *in vivo* rate obtained at 100 mM  $[\text{NO}_3^-]_o$  for a 20-min incubation, which was approximately  $1 \mu\text{mol g}^{-1}$  fresh weight  $\text{h}^{-1}$ .

The NADH-dependent activity was much higher than the NADPH-dependent activity, accounting for approximately 80% of the total at high  $\text{NO}_3^-$  concentrations. Its  $K_m$  value was 1.41 mM (Fig. 4). The NADPH-dependent activity showed a considerably higher  $\text{NO}_3^-$  affinity, with a  $K_m$  for  $\text{NO}_3^-$  of 0.16 mM (Fig. 4).

These values differ considerably from those previously reported. For leaves of barley cv Steptoe, Dailey *et al.* (7) obtained values of 0.13 and 1.2 mM for the NADH and NAD(P)H enzymes, respectively, and Harker *et al.* (14) obtained a value of 0.61 mM for the NAD(P)H enzyme. Typically,  $K_m$  values of approximately 0.2 mM have been obtained for the NADH enzyme from several plant species (13). The reason for the difference between our results and those of previous studies is not clear. However, considerable interspecific variation appears to occur among  $K_m$  values for both enzyme forms (12), and the previous investigators have used leaves rather than roots. It seems reasonable that differences might occur between roots and leaves and among cultivars of the same species.

### Estimation of $[\text{NO}_3^-]_c$

If it can be assumed that the *in vivo* kinetic parameters and relative magnitudes of the NADH- and NADPH-dependent activities are similar to those determined *in vitro*, then two conclusions can be drawn. First, given the low  $K_m$  of the NADPH-dependent activity, it is likely that this activity *in vivo* is always  $\text{NO}_3^-$  saturated (compare Figs. 2 and 3). At low  $[\text{NO}_3^-]_o$  (0–2 mM), it would account for approximately 50% of the *in vivo* activity shown in Figure 2; whereas at high  $[\text{NO}_3^-]_o$  (20–50 mM), it would account for approximately 20%. Second, due to its lower  $\text{NO}_3^-$  affinity and higher relative activity, the NADH-dependent activity likely accounts for most, if not all, of the response to increased  $[\text{NO}_3^-]_o$  shown in Figure 2. Therefore, we based our calculation of  $[\text{NO}_3^-]_c$  on the NADH-dependent activity, after correcting the *in vivo* data shown in Figure 2 for the estimated NADPH-dependent activity as seen in Figure 3. Figure 5 shows the estimates for  $[\text{NO}_3^-]_c$  with increasing  $[\text{NO}_3^-]_o$ . At zero  $[\text{NO}_3^-]_o$ ,  $[\text{NO}_3^-]_c$  was 0.66 mM, and it increased in an approximately linear fashion with  $[\text{NO}_3^-]_o$ , reaching 3.9 mM at 20 mM  $[\text{NO}_3^-]_o$ . At higher  $[\text{NO}_3^-]_o$  values,  $[\text{NO}_3^-]_c$  could not be calculated directly from the data shown in Figure 2, due to saturation of the NADH-dependent activity. However, if the linear relationship holds for higher values of  $[\text{NO}_3^-]_o$ , then at 100 mM (which gave the maximum *in vivo* NRA),  $[\text{NO}_3^-]_c$  would be approximately 17 mM.

Recently, Zhen *et al.* (33), using  $\text{NO}_3^-$ -specific microelec-

trodes, estimated  $[\text{NO}_3^-]_c$  to be 5.4 and 3.2 mM, respectively, for epidermal and cortical root cells of barley plants grown in 10 mM  $\text{NO}_3^-$ . The two values were judged not to be significantly different. This result would appear to contradict the suggestion of Siddiqi *et al.* (29) that  $[\text{NO}_3^-]_c$  is higher in the cortical cells than in the epidermal cells (see the introduction). However, growth in 10 mM  $\text{NO}_3^-$  (in contrast with 100  $\mu\text{M}$  as used in our studies) may have elevated  $[\text{NO}_3^-]_c$  in the epidermal cells to a level that saturates NR, eliminating any difference between the two cell types. In any case, the results of Zhen *et al.* (33) are consistent with our observation that  $[\text{NO}_3^-]_c$  is in the low millimolar range for values of  $[\text{NO}_3^-]_o$  from 5 to 20 mM (Fig. 5).

Our results support those of Siddiqi *et al.* (29) using compartmental analysis, which show that  $[\text{NO}_3^-]_c$  increases with increasing  $[\text{NO}_3^-]_o$ , although compartmental analysis yields much higher values (see the introduction). Siddiqi *et al.* (29) suggested that  $[\text{NO}_3^-]_c$  is not as rigorously controlled as cytoplasmic concentrations of other major ions such as  $\text{K}^+$  and Pi. This seems reasonable because  $\text{NO}_3^-$ , unlike these ions, does not directly regulate cellular metabolism (except for the induction of  $\text{NO}_3^-$  transport and NR). Although varying  $[\text{NO}_3^-]_c$  would have effects on charge and osmotic balance, presumably these could be compensated for by other solute fluxes.

### Implications for $\text{NO}_3^-$ Influx

Figure 6 shows the relationship between  $[\text{NO}_3^-]_c$  and  $E^N$  for four different values of  $[\text{NO}_3^-]_o$ , calculated according to the Nernst equation, which assumes passive equilibration of  $\text{NO}_3^-$  across the plasma membrane, in which case  $\Delta\Psi$  is equivalent to  $E^N$ . The  $E^N$  values span the range of measured  $\Delta\Psi$  values for barley as determined by Glass *et al.* (10) (–200 to –300 mV) as well as including less negative values. Given our estimates of  $[\text{NO}_3^-]_c$  (between 0.6 and 1 mM for  $[\text{NO}_3^-]_o$  values between 0.1 and 1 mM; Fig. 5), it is clear that passive  $\text{NO}_3^-$  influx via the LATS could not occur at  $\Delta\Psi$  values between –200 and –300 mV. At such values,  $[\text{NO}_3^-]_c$  would have to be in the nanomolar range (10).

The values that have been previously obtained for  $\Delta\Psi$  of barley root cells are rather variable. For example, Mertz and Higinbotham (22) obtained values between –100 and –200 mV, and Zhen *et al.* (33) recently obtained a mean value of approximately –70 mV, considerably less negative than the values obtained by Glass *et al.* (10). The reason for the difference between the results of these studies is not clear. However, given a  $\Delta\Psi$  value of –70 mV and our estimates of  $[\text{NO}_3^-]_c$ , passive net entry of  $\text{NO}_3^-$  via the LATS is still not possible except at very high  $[\text{NO}_3^-]_o$  (approximately 10 mM).

The use of a  $K_m$  of 0.13 mM for the NADH enzyme, as obtained by Dailey *et al.* (7), rather than our value of 1.4 mM, yields lower values for  $[\text{NO}_3^-]_c$ , e.g. 60  $\mu\text{M}$  at zero  $[\text{NO}_3^-]_o$ . With such values, at a  $\Delta\Psi$  of approximately –70 mV as obtained by Zhen *et al.* (33), influx of  $\text{NO}_3^-$  via the LATS could be passive (Fig. 6). However, we consider such an extreme scenario unlikely for several reasons. First, the agreement between our *in vivo* and *in vitro* data for  $\text{NO}_3^-$  concentration dependence of NRA suggests that the  $K_m$  value we obtained, although different from those of other studies, is

correct for the barley cultivar we used. Second, in our analysis, we used kinetic parameters and  $\Delta\Psi$  values from the same cultivar grown to the same age under similar conditions. Finally, consistent with our observations, the depolarization of  $\Delta\Psi$  observed by Glass *et al.* (10) strongly suggests that the LATS is an active system.

### CONCLUSIONS

Determination of  $[\text{NO}_3^-]_c$  in barley roots using the NR-based method of Robin *et al.* (25) yields values of approximately 0.6 to 1 mM for 0.1 to 1 mM  $[\text{NO}_3^-]_o$ , in contrast to the values of 12 to 37 mM obtained by compartmental analysis (29). The present findings support the proposal of Siddiqi *et al.* (29) that the two techniques measure  $[\text{NO}_3^-]_c$  in two different pools; respectively, a large, slowly metabolized pool (possibly the cytoplasm of the cortical cells) and a smaller, NR-containing, actively metabolized pool (possibly the cytoplasm of the epidermal cells).

$[\text{NO}_3^-]_c$  increased with increasing  $[\text{NO}_3^-]_o$ , up to 3.9 mM at 20 mM  $[\text{NO}_3^-]_o$ , confirming the results of Siddiqi *et al.* (29) from compartmental analysis and supporting their suggestion that  $[\text{NO}_3^-]_c$  is not as closely regulated as the cytoplasmic pools of other major ions.

At the values we obtained for  $[\text{NO}_3^-]_c$ , passive transport via the LATS is essentially impossible given the  $\Delta\Psi$  values measured by Glass *et al.* (10). Our results support their suggestion that the LATS is energetically active. Nevertheless, the LATS shows characteristics that are very puzzling for an active system, including linear kinetics, lower sensitivity to metabolic inhibitors than the HATS, and a lower temperature coefficient (11, 31). The paradoxical characteristics of this transport system clearly warrant further investigation.

### ACKNOWLEDGMENTS

We wish to thank Jarnail Mehroke, Miaoyuan Wang, and Dr. Ann Oaks for assistance and useful discussion.

### LITERATURE CITED

- Aslam M (1981) Reevaluation of anaerobic nitrite production as an index for the measurement of metabolic pool of nitrate. *Plant Physiol* 68: 305–308
- Beevers L, Hageman RH (1980) Nitrate and nitrite reduction. In BJ Mifflin, ed, *The Biochemistry of Plants*, Vol 5: Amino Acids and Derivatives. Academic Press, New York, pp 115–168
- Belton PS, Lee RB, Ratcliffe RG (1985) A  $^{14}\text{N}$  nuclear magnetic resonance study of inorganic nitrogen metabolism in barley, maize and pea roots. *J Exp Bot* 36: 190–210
- Brunetti N, Hageman RH (1976) Comparison of *in vivo* and *in vitro* assays of nitrate reductase in wheat (*Triticum aestivum* L.) seedlings. *Plant Physiol* 58: 583–587
- Cataldo DA, Haroon M, Schrader LE, Youngs VL (1975) Rapid colorimetric determination of nitrate in plant tissue by nitration of salicylic acid. *Commun Soil Sci Plant Anal* 6: 71–80
- Clarkson DT (1986) Regulation of the absorption and release of nitrate by plant cells: a review of current ideas and methodology. In H Lambers, JJ Neeteson, I Stulen, eds, *Fundamental, Ecological and Agricultural Aspects of Nitrogen Metabolism in Higher Plants*. Martinus Nijhoff, Boston, MA, pp 3–27
- Dailey FA, Warner RL, Somers DA, Kleinhofs A (1982) Characteristics of a nitrate reductase in a barley mutant deficient in NADH nitrate reductase. *Plant Physiol* 69: 1200–1204
- Deane-Drummond CE, Glass ADM (1982) Nitrate uptake into barley (*Hordeum vulgare*) plants. A new approach using  $^{36}\text{ClO}_3^-$  as an analogue for  $\text{NO}_3^-$ . *Plant Physiol* 70: 50–54
- Ferrari TE, Yoder OC, Filner P (1973) Anaerobic nitrite production by plant cells and tissues. Evidence for two nitrate pools. *Plant Physiol* 51: 423–431
- Glass ADM, Schaff JE, Kochian LV (1992) Studies of the uptake of nitrate in barley. IV. Electrophysiology. *Plant Physiol* 99: 456–463
- Glass ADM, Siddiqi MY, Ruth TJ, Rufty TW Jr (1990) Studies of the uptake of nitrate in barley. II. Energetics. *Plant Physiol* 93: 1585–1589
- Guerrero MG, Vega JM, Losada M (1981) The assimilatory nitrate-reducing system and its regulation. *Annu Rev Plant Physiol* 32: 169–204
- Hageman RH, Reed AJ (1980) Nitrate reductase from higher plants. *Methods Enzymol* 69: 270–280
- Harker AR, Komaratchi RN, Warner RL, Kleinhofs A (1986) NAD(P)H bispecific nitrate reductase in barley leaves: partial purification and characterization. *Phytochemistry* 25: 1275–1279
- Hedrich R, Schroeder JI (1989) The physiology of ion channels and electrogenic pumps in higher plants. *Annu Rev Plant Physiol* 40: 539–569
- Jordan DB, Fletcher JS (1980) Nitrate assimilation in suspension cultures of Paul's Scarlet rose. *Can J Bot* 58: 1088–1094
- Kuo T-M, Kleinhofs A, Warner RL (1982) *In vitro* stability of nitrate reductase from barley leaves. *Phytochemistry* 25: 1275–1279
- Lee RB, Clarkson DT (1986) Nitrogen-13 studies of nitrate fluxes in barley roots. I. Compartmental analysis from measurements of  $^{13}\text{N}$  efflux. *J Exp Bot* 37: 1753–1767
- Long DM, Oaks A (1990) Stabilization of nitrate reductase in maize roots by chymostatin. *Plant Physiol* 93: 846–850
- Macklon AES, Ron MM, Sim A (1990) Cortical cell fluxes of ammonium and nitrate in excised root segments of *Allium sepa* L.; studies using  $^{15}\text{N}$ . *J Exp Bot* 41: 359–370
- McKown CT, Jackson WA, Volk RJ (1983) Partitioning of previously-accumulated nitrate to translocation, reduction, and efflux in corn roots. *Planta* 157: 8–14
- Mertz SM Jr, Higinbotham M (1976) Transmembrane electro-potential in barley roots as related to cell type, cell location, and cutting and aging effects. *Plant Physiol* 57: 123–128
- Miller AJ, Zhen R-G (1991) Measurement of intracellular nitrate concentrations in *Chara* using nitrate-selective microelectrodes. *Planta* 184: 47–52
- Presland MR, McNaughton GS (1984) Whole plant studies using radioactive 13-nitrogen. II. A compartmental model for the uptake and transport of nitrate ions by *Zea mays*. *J Exp Bot* 35: 1277–1288
- Robin P, Conejero G, Passama L, Salsac L (1983) Evaluation de la fraction métabolisable du nitrate par la mesure *in situ* de sa réduction. *Physiol Veg* 21: 115–122
- Robin P, Conejero G, Tranchant J-P, Passama L, Salsac L (1983) Mesure de la réduction du nitrate dans les feuilles intactes. *Physiol Veg* 21: 123–128
- Rufty TW Jr, Thomas JF, Remmler JL, Campbell WH, Volk RJ (1986) Intercellular localization of nitrate reductase in roots. *Plant Physiol* 82: 675–680
- Siddiqi MY, Glass ADM (1987) Regulation of  $\text{K}^+$  influx in barley: evidence for a direct control of influx by  $\text{K}^+$  concentration of root cells. *J Exp Bot* 38: 935–947
- Siddiqi MY, Glass ADM, Ruth TJ (1991) Studies of the uptake of nitrate in barley. III. Compartmentation of  $\text{NO}_3^-$ . *J Exp Bot* 42: 1455–1463
- Siddiqi MY, Glass ADM, Ruth TJ, Fernando M (1989) Studies of the regulation of nitrate influx by barley seedlings using  $^{13}\text{NO}_3^-$ . *Plant Physiol* 90: 806–813
- Siddiqi MY, Glass ADM, Ruth TJ, Rufty TW Jr (1990) Studies of the uptake of nitrate in barley. I. Kinetics of  $^{13}\text{NO}_3^-$  influx. *Plant Physiol* 93: 1426–1432
- Warner RL, Huffaker RC (1989) Nitrate transport is independent of NADH and NAD(P)H nitrate reductases in barley seedlings. *Plant Physiol* 91: 947–953
- Zhen R-G, Koyro HW, Leigh RA, Tomos AD, Miller AJ (1991) Compartmental nitrate concentrations in barley root cells measured with nitrate-selective microelectrodes and by single-cell sap sampling. *Planta* 185: 356–361